

Research paper

Particle tracking in ideal faulted blocks using 3D co-ordinate geometry

Soumyajit Mukherjee

Department of Earth Sciences, Indian Institute of Technology Bombay, Powai, Mumbai 400 076, Maharashtra, India



ARTICLE INFO

Keywords:

Brittle deformation
Slip along planes
Rotation in structural geology
Deformation modeling
Tribology

ABSTRACT

This article performs particle (/material point) tracking for ideal brittle faults with translational and rotational slip components. The fault planes are considered to be planar and step-like in separate cases. In the latter case the hangingwall block is considered to behave ductilely. For a specific choice of the three Cartesian co-ordinate axes, dip-slip fault will change two out of the three ordinates of any point in the faulted block that moves. A strike slip faulting can change one out of the three ordinates. On the other hand, whatever be the orientation of the orthogonal co-ordinate axes, an oblique slip fault of any dip amount and a purely rotational fault with dip $\neq 0, 90^\circ$ alter all the three ordinates, except the pivot point in the latter case. As expected, oblique-slip faulting modifies the co-ordinates of the shifted material points depending on both (i) the pitch of stretching lineation, and (ii) the dip of the fault plane.

1. Introduction

Understanding the geometry and the kinematics of faults (e.g., Billings, 1972; Mukherjee 2018; Mukherjee and Khonsari, 2018; Mukherjee and Tayade, in press), especially involving their ramp-flat geometry, are of great importance in petroleum geosciences (e.g., Kent et al., 2002). To achieve these goals, faulted blocks are restored while balancing structural cross-sections (Lopez-Mir, 2019). One way to achieve this would be to develop a particle tracking method, before and after deformation. Particle tracking is popular in other disciplines of deformation modeling (Ando et al., 2012). Standard numerical techniques have been implemented in structural geological problems in 2D and 3D (e.g., Groshong, 2006; Allmendinger et al., 2012).

Fault planes can widely vary in dip amounts. Vertical fault planes were conceptualized to explain various isostasy models (Turcotte and Schubert, 2002; Mukherjee, 2017). Apart from such theoretical models, vertical and sub-vertical fault planes have also been documented from several terrains (e.g., Misra et al., 2014) that can be linked with either isostasy or strike-slip tectonics as a part of positive or negative flower structures (Dasgupta and Mukherjee, 2017). Likewise, (sub)horizontal faults and shear zones have been documented from numerous terrains, usually at the boundary between the upper and the lower crust based on geophysical studies (e.g., Kobayashi et al., 2018).

Ramps develop in mechanically incompetent layers, whereas flats appear inside the competent lithology (Merle, 1998). Ramp and flat geometry of reverse faults are quite common in collisional mountain belts and constitutes an integral part of fault-bend and fault propagation folding (review in Mukherjee, 2013). Ramps dip typically 35 to 40°

and connote a thin-skinned tectonics (Boyer and Elliot, 1982). Savage and Cooke (2003) in their numerical models consider this dip to range 30 to 75°. While a “flat-ramp-flat” geometry is fairly common for fault planes (Davis et al., 2012), geometries such as “ramp-flat-ramp” (SE Spain: Ehrlich and Gabrielsen, 2004; Padrera et al., 2012) and “flat-ramp-flat-ramp” (west Taiwan: Lock, 2007) have also been reported. A ramp-flat geometry of normal faults in an extensional tectonic regime is also possible (Gibbs, 1984), though presumably uncommon. In such a setting, an extensional imbricate structure develops over the normal fault plane (Fossen, 2016). The hangingwall block in case of fault planes with steps can be deformable and behave in a ductile manner (e.g., Rodriguez-Castaneda, 1996; especially McClay, 1990 for extensional fault systems) and progressively collapse on the fault plane (Fossen, 2016) thereby avoiding any space-problem that may otherwise arise in such faulting.

To the author's knowledge, strike-slip fault planes with ramp-flat geometry do not exist. However, bends of both releasing and restraining types and offset noted in plan view are well established in strike-slip faults (Cunningham and Mann, 2007). Mostly the strike-slip faults are (sub)vertical, as expected from Anderson's theory of faulting. Sometimes however, steeply dipping strike-slip faults have been reported (Nemser and Kowan, 2009), and more rarely these fault planes can be low-dipping (Huetra and Rodgers, 1996).

This article makes a simple analysis to track points before and after the brittle deformation for ideal translational and rotational fault types with planar fault planes. Real faults can be more complicated and would require additional numerical care. Simplified approaches of fault block restoration (without using co-ordinate geometry) are noted also

E-mail addresses: soumyajitm@gmail.com, smukherjee@iitb.ac.in.

<https://doi.org/10.1016/j.marpetgeo.2019.05.037>

Received 4 January 2019; Received in revised form 17 May 2019; Accepted 29 May 2019

Available online 01 June 2019

0264-8172/ © 2019 Elsevier Ltd. All rights reserved.

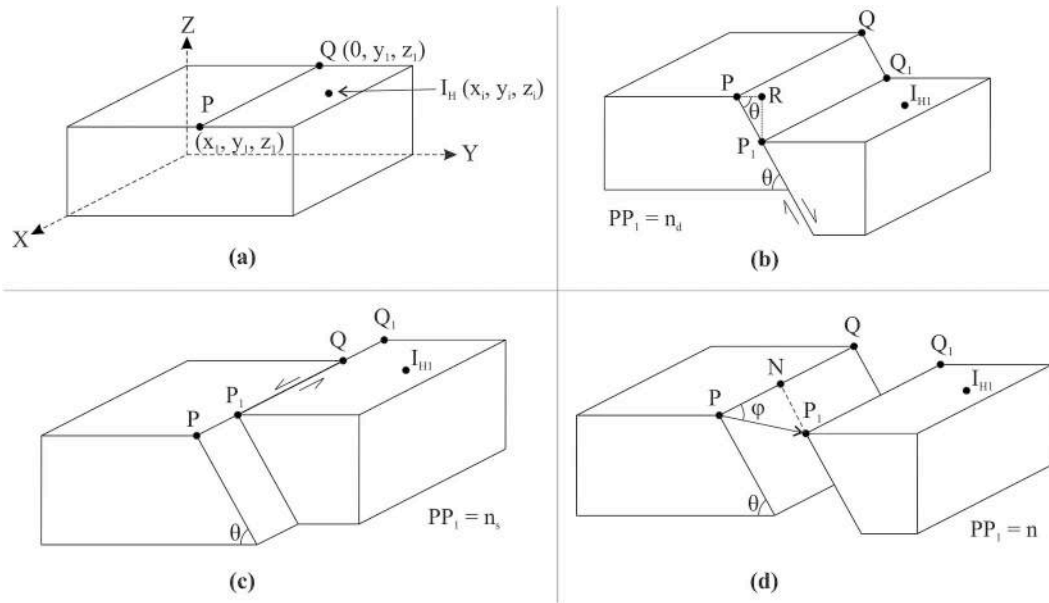


Fig. 1. a. A rectangular parallelepiped with chosen Cartesian co-ordinate system (Sections 2.1.1). PQ is the surface trace of a future fault. P is (x_1, y_1, z_1) and Q is $(0, y_1, z_1)$. $I_H(x_i, y_i, z_i)$ is any point in the future hanging wall block of the fault. $y_i > y_1$. I_{H1} is the position of I_H after faulting. b. A dip-slip normal fault (Section 2.1.1). Fault plane dips at θ towards the positive side of the Y-axis. Net-slip = dip-slip = $PP_1 = n_d$. Heave = $h = PR$, throw = $t = RP_1$. c. Sinistral strike-slip fault (Section 2.1.1.2). Net-slip = strike-slip = $PP_1 = n_s$. d. Oblique-slip normal fault with a sinistral strike-slip component (Section 2.1.1.3). Net-slip = $PP_1 = n$.

in cross-section balancing exercises (Lopez-Mir, 2019).

2. Model

Consider a rectangular parallelepiped of rock(s) and the Cartesian co-ordinate axes as per Fig. 1a. Points P and Q have co-ordinates $[r_i]$ ($r = x, y, z$) and $[0, y_1, z_1]$, respectively. Consider different types of faulting on this block in distinct cases with the line PQ as the surface trace or the strike line of the future fault. The equation of the line PQ can be deduced.

The planar fault plane dips at an angle of θ (Fig. 1b) towards the right hand side, i.e., towards the positive side of the Y-axis. The fault plane trends along the X-axis and has the equation:

$$z = y \cdot \tan \theta - d \cdot c^{-1} \tag{1}$$

See Repository for derivation.

Lets start from the simple types of faulting and progressively address the more complicated cases. Both the hangingwall block and the footwall block may undergo absolute slip in real cases. To deduce the co-ordinate of shifted points due to faulting, this work however considers one of the faulted blocks to be stationary. The same approach has been noted in the published articles in structural geology and tectonics (Ghosh, 1993). For modeling purpose, one of the blocks is kept stationary in analogue models (e.g., simple shear models with one of the shear zone walls stationary: Cobbold and Quinquis, 1980), numerical models (e.g., pure shear model with one of the shear zone walls stationary: Mukherjee, 2019), and in cross-section balancing tutorials (Marshak and Mitra, 1988).

2.1. Translational faults

2.1.1. Faults with a single planar fault surface

2.1.1.1. Dip-slip faults. In case of dip-slip normal faults (Fig. 1b), if the faulted blocks are restored, say point P_1 in the hangingwall block would superpose with the point P in the footwall block. Net-slip = distance $PP_1 = n_d$, say. Construct triangle PRP_1 with the angle $PRP_1 = 90^\circ$. Therefore, heave (h) = $PR = n_d \cdot \cos \theta$, and throw (t) $RP_1 = n_d \cdot \sin \theta$. Therefore co-ordinate of P_1 :

$$[x_i, y_1 + n_d \cdot \cos \theta, z_1 - n_d \cdot \sin \theta] \tag{2}$$

For any co-ordinate $[r_i]$, ($r = x, y, z$) for the point I_H before faulting and within the future hangingwall block, its co-ordinate I_{H1} after faulting becomes

$$[x_i, y_i + n_d \cdot \cos \theta, z_i - n_d \cdot \sin \theta] \tag{3}$$

Since the footwall block is considered stationary, coordinates of all points inside it remains the same after faulting. If the hangingwall block remains stationary and the footwall block move upward, any point inside the footwall block $I_F [r_i]$, ($r = x, y, z$) would attain the new co-ordinate I_{F1} :

$$[x_i, y_i - n_d \cdot \cos \theta, z_i + n_d \cdot \sin \theta] \tag{4}$$

In case of dip-slip reverse faults, if the footwall block only moves, I_{F1} :

$$[x_i, y_i + n_d \cdot \cos \theta, z_i - n_d \cdot \sin \theta] \tag{5}$$

And if the hangingwall block only moves, I_{H1} :

$$[x_i, y_i - n_d \cdot \cos \theta, z_i + n_d \cdot \sin \theta] \tag{6}$$

Since no movement takes place along the fault strike, here the X-direction, the x-ordinate (x_1) remains the same in all these cases.

2.1.1.2. Strike-slip fault. For a sinistral strike-slip fault (Fig. 1c), if the hangingwall block moved with net-slip = n_s , P_1 :

$$[x_1 - n_s, y_1, z_1] \tag{7}$$

Therefore I_{H1} is:

$$[x_i - n_s, y_i, z_i] \tag{8}$$

If the footwall block only moved, I_{F1} is:

$$[x_i + n_s, y_i, z_i] \tag{9}$$

For a dextral fault, if the hangingwall block only moved, I_H :

$$[x_i + n_s, y_i, z_i] \tag{10}$$

Whereas, in case only the footwall block moved, I_{H1} :

$$[x_i - n_s, y_i, z_i] \tag{11}$$

In both the sinistral and the dextral cases, only the X-ordinates (x_i) change and the other two ordinates (y_i and z_i) remain the same. This is just the opposite case of the dip-slip faults. Also note that the new co-ordinate is independent of the dip (θ) of the fault plane.

2.1.1.3. Oblique-slip faults. In case of an oblique-slip normal fault with sinistral slip component (Fig. 1d) with “ Φ ” as the pitch or the rake, and “ n ” as the net-slip. Construct triangle PNP_1 where the angle $PNP_1 = 90^\circ$. Here $PN = n_s = n \cos \Phi$; and $NP_1 = n_d = n \sin \Phi$. Two well known relations are as follow:

$$n^2 = n_d^2 + n_s^2 \tag{12}$$

$$\tan \Phi = n_d n_s^{-1} \tag{13}$$

The horizontal component of n_d , along the positive direction of the Y-axis, equals $n_d \cos \theta = n \sin \Phi \cos \theta$. The vertical component of n_d , along the Z-axis direction, equals $n_d \sin \theta = n \sin \Phi \sin \theta$. Therefore the co-ordinate I_{H1} , if only the hangingwall block move, is:

$$[x_i - n \cos \Phi, y_i + n \cos \theta \sin \Phi, z_i - n \sin \Phi \sin \theta] \tag{14}$$

For an oblique-slip normal fault with dextral slip component, if only the hangingwall block move, I_{H1} is:

$$[x_i + n \cos \Phi, y_i + n \cos \theta \sin \Phi, z_i - n \sin \Phi \sin \theta] \tag{15}$$

If only the footwall block move, I_{F1} :

$$[x_i - n \cos \Phi, y_i + n \cos \theta \sin \Phi, z_i - n \sin \Phi \sin \theta] \tag{16}$$

In case only the footwall had moved for an oblique-slip reverse fault with sinistral slip, I_{F1} is:

$$[x_i + n \cos \Phi, y_i - n \cos \theta \sin \Phi, z_i + n \sin \Phi \sin \theta] \tag{17}$$

If the same sense of faulting happened by moving only the hangingwall block, I_{H1} is:

$$[x_i - n \cos \Phi, y_i + n \cos \theta \sin \Phi, z_i - n \sin \Phi \sin \theta] \tag{18}$$

2.1.2. Fault planes with step-geometries

2.1.2.1. Dip-slip fault. Suppose the “fault plane” can be divided into

two distinct planar surfaces FP-1 and FP-2 of same dip direction but with different dip amounts θ_1 and θ_2 ($\theta_1 > \theta_2$; Fig. 2a1). Consider that the net-slip “ n ” is divided into “ n_1 ” and “ n_2 ” on FP-1 and FP-2, respectively. This means,

$$n = n_{d1} + n_{d2} \tag{19}$$

Consider the triangle PP_1P_2 that is vertical to the XY horizontal plane. Here angle $PP_1P_2 = (180^\circ + \theta_2 - \theta_1)$. Say the P co-ordinate is (x_i, y_i, z_i). Applying exp (2) on n_{d1} , if only the hangingwall block moved, the P_1 co-ordinate is:

$$[x_i, y_i + n_{d1} \cos \theta_1, z_i - n_{d1} \sin \theta_1] \tag{20}$$

Putting these r_1 ($r = x, y, z$) values in exp (2) again, for the next slip along the FP-2, P_2 is given by:

$$[x_i, y_i + n_{d1} \cos \theta_1 + n_{d2} \cos \theta_2, z_i - n_{d1} \sin \theta_1 - n_{d2} \sin \theta_2] \tag{21}$$

Therefore, I_{H1} :

$$[x_i, y_i + n_{d1} \cos \theta_1 + n_{d2} \cos \theta_2, z_i - n_{d1} \sin \theta_1 - n_{d2} \sin \theta_2] \tag{22}$$

And I_{F1} ,

$$[x_i, y_i - n_{d1} \cos \theta_1 - n_{d2} \cos \theta_2, z_i + n_{d1} \sin \theta_1 + n_{d2} \sin \theta_2] \tag{23}$$

For “ m ” number of steps in the fault, I_{Hm} :

$$[x_i, y_i + \sum n_{dj} \cos \theta_j, z_i - \sum n_{dj} \sin \theta_j] \quad (j=1 \text{ to } m) \tag{24}$$

Similarly, I_{Fm} :

$$[x_i, y_i - \sum n_{dj} \cos \theta_j, z_i + \sum n_{dj} \sin \theta_j] \quad (j=1 \text{ to } m) \tag{25}$$

For a dip-slip reverse fault with steps, exp (21) and (22) become, respectively,

$$[I_{Hm}: x_i, y_i - \sum n_{dj} \cos \theta_j, z_i + \sum n_{dj} \sin \theta_j] \quad (j=1 \text{ to } m) \tag{26}$$

$$[I_{Fm}: x_i, y_i + \sum n_{dj} \cos \theta_j, z_i - \sum n_{dj} \sin \theta_j] \quad (j=1 \text{ to } m) \tag{27}$$

2.1.2.2. Strike-slip fault. With reference to Fig. 2b, even if such a fault plane really exists and consists of steps, the shifted co-ordinate has the same expressions as that of a strike-slip fault plane that is devoid of any stems (such as exps. (7)–(11)):

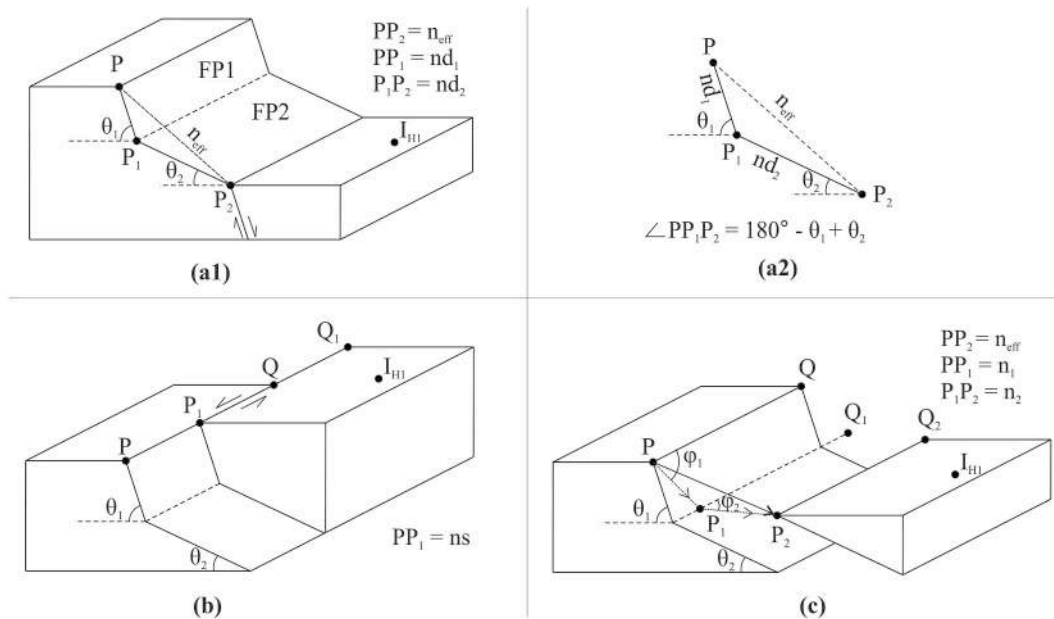


Fig. 2. Fault plane with steps (Section 2.1.2). I_{H1} is the position of I_H (x_i, y_i, z_i) after faulting. **a1.** Dip-slip normal fault (Section 2.1.2.1). FP-1 dips at θ_1 and FP-2 at θ_2 . $PP_1 = n_{d1}$, $PP_2 = n_{d2}$. $PP_2 = n_{eff}$. **a2.** The PP_1P_2 triangle is drawn separately to calculate n_{eff} . **b.** Sinistral strike-slip fault (Section 2.1.2.2). Net-slip = strike-slip = n_s . **c.** Oblique-slip normal fault with sinistral strike-slip components on FP-1 and FP-2 (Section 2.1.2.3). Net slip (n) = ($PP_1 + P_1P_2$) = ($n_1 + n_2$). Angle QPP_1 lying on FP-1 = ϕ_1 ; angle $Q_1P_1P_2$ lying on FP-2 = ϕ_2 .

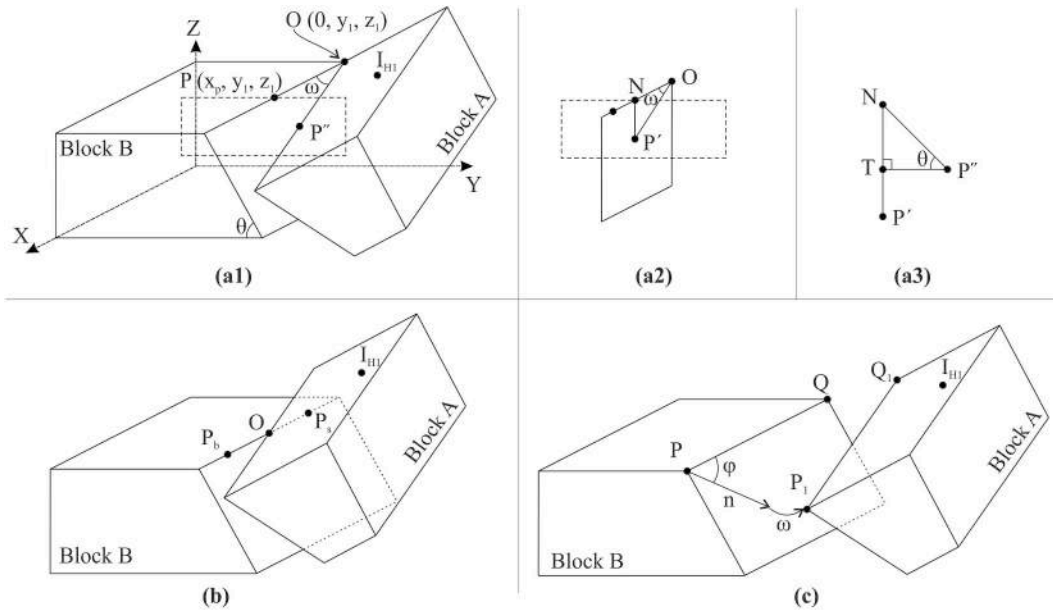


Fig. 3. Fault with rotational component (Section 2.2). **a1.** A purely rotational fault (Section 2.2.1). The pivot O is located at the end point of the fault trace. Point P after faulting shifts to P'. **a2.** The plane parallel to XZ-plane passing through the line PO (drawn by dash lines in Fig. 3a1) is drawn separately. **a3.** The plane parallel to the YZ-plane passing through the point N (drawn by dash lines in Fig. 3a2) is drawn separately. **b.** A purely rotational fault with the pivot O lying on and in between the two ends of the fault trace (Section 2.2.1). **c.** A roto-translational fault with translational net-slip = n, and ω amount of rotation (Section 2.2.2).

For a sinistral fault,

$$I_{H1}: [x_i - n_s, y_i, z_i] \quad (28)$$

$$I_{F1}: [x_i + n_s, y_i, z_i] \quad (29)$$

For a dextral fault

$$I_{H1}: [x_i + n_s, y_i, z_i] \quad (30)$$

$$I_{F1}: [x_i - n_s, y_i, z_i] \quad (31)$$

2.1.2.3. Oblique-slip fault. Consider an oblique-slip normal fault with sinistral slip along both the fault steps FP-1 and FP-2 (Fig. 2c). Unlike the previous cases of dip-slip faults, here the PP₁P₂ plane is not perpendicular to the fault plane strike. Say the pitch of net-slip vector on FP-1 and FP-2 are Φ₁ and Φ₂, respectively.

The strike-slip component of n₁ and n₂ on FP-1 and FP-2 are n_{s1} = n₁cosΦ₁ and n_{s2} = n₂cosΦ₂, respectively. Therefore The total strike-slip component, along the X axis is, n_s = (n_{s1} + n_{s2}) = (n₁cosΦ₁ + n₂cosΦ₂). The dip-slip component of n₁ and n₂ on FP-1 and FP-2 are n_{d1} = n₁sinΦ₁ and n_{d2} = n₂sinΦ₂, respectively. Therefore, the heave of the n_{d1} and the n_{d2} components on FP-1 and FP-2 are h₁ = n_{d1}cosθ₁ = n₁sinΦ₁.cosθ₁, and h₂ = n_{d2}cosθ₂ = n₂sinΦ₂.cosθ₂, respectively. Likewise, the throw of the n_{d1} and the n_{d2} components on FP-1 and FP-2 are t₁ = n_{d1}.sinθ₁ = n₁sinΦ₁.sinθ₁ and t₂ = n₂sinΦ₁.sinθ₂, respectively. Therefore, the total horizontal component of net-slip, along the Y-axis is, h = (n₁sinΦ₁.cosθ₁ + n₂sinΦ₂.cosθ₂), and the total vertical component of net-slip t = (n₁cosΦ₁.cosθ₁ + n₂cosΦ₂.cosθ₂). Therefore, P₂ has the co-ordinate:

$$\begin{aligned} & [x_i - (n_1\cos\Phi_1 + n_2\cos\Phi_2), y_i + (n_1\sin\Phi_1.\cos\theta_1 + n_2\sin\Phi_2.\cos\theta_2), \\ & z_i - (n_1\cos\Phi_1.\cos\theta_1 + n_2\cos\Phi_2.\cos\theta_2)] \end{aligned} \quad (32)$$

Any point I_H [r_i] (i = x, y, z) before faulting will have the coordinate after faulting I_{H1}:

$$\begin{aligned} & [x_i - (n_1\cos\Phi_1 + n_2\cos\Phi_2), y_i + (n_1\sin\Phi_1.\cos\theta_1 + n_2\sin\Phi_2.\cos\theta_2), \\ & z_i - (n_1\cos\Phi_1.\cos\theta_1 + n_2\cos\Phi_2.\cos\theta_2)] \end{aligned} \quad (33)$$

And, I_{F1}:

$$\begin{aligned} & [x_i + (n_1\cos\Phi_1 + n_2\cos\Phi_2), y_i - (n_1\sin\Phi_1.\cos\theta_1 + n_2\sin\Phi_2.\cos\theta_2), \\ & z_i + (n_1\cos\Phi_1.\cos\theta_1 + n_2\cos\Phi_2.\cos\theta_2)] \end{aligned} \quad (34)$$

In case this oblique-slip fault had a sinistral component of strike-slip on FP-1, and a dextral component of strike-slip on FP-2, then I_{H1}:

$$\begin{aligned} & [x_i - (n_1\cos\Phi_1 - n_2\cos\Phi_2), y_i + (n_1\sin\Phi_1.\cos\theta_1 + n_2\sin\Phi_2.\cos\theta_2), \\ & z_i - (n_1\cos\Phi_1.\cos\theta_1 + n_2\cos\Phi_2.\cos\theta_2)] \end{aligned} \quad (35)$$

If this oblique-slip fault had dextral slip component on both FP-1 and FP-2: I_{H1}:

$$\begin{aligned} & [x_i + (n_1\cos\Phi_1 + n_2\cos\Phi_2), y_i + (n_1\sin\Phi_1.\cos\theta_1 + n_2\sin\Phi_2.\cos\theta_2), \\ & z_i - (n_1\cos\Phi_1.\cos\theta_1 + n_2\cos\Phi_2.\cos\theta_2)] \end{aligned} \quad (36)$$

And I_{F1}:

$$\begin{aligned} & [x_i - (n_1\cos\Phi_1 + n_2\cos\Phi_2), y_i - (n_1\sin\Phi_1.\cos\theta_1 + n_2\sin\Phi_2.\cos\theta_2), \\ & z_i + (n_1\cos\Phi_1.\cos\theta_1 + n_2\cos\Phi_2.\cos\theta_2)] \end{aligned} \quad (37)$$

For an oblique-slip reverse fault with sinistral slip component.

I_{H1}:

$$\begin{aligned} & [x_i + (n_1\cos\Phi_1 + n_2\cos\Phi_2), y_i - (n_1\sin\Phi_1.\cos\theta_1 + n_2\sin\Phi_2.\cos\theta_2), \\ & z_i + (n_1\cos\Phi_1.\cos\theta_1 + n_2\cos\Phi_2.\cos\theta_2)] \end{aligned} \quad (38)$$

I_{F1}:

$$\begin{aligned} & [x_i - (n_1\cos\Phi_1 + n_2\cos\Phi_2), y_i + (n_1\sin\Phi_1.\cos\theta_1 + n_2\sin\Phi_2.\cos\theta_2), \\ & z_i - (n_1\cos\Phi_1.\cos\theta_1 + n_2\cos\Phi_2.\cos\theta_2)] \end{aligned} \quad (39)$$

For “m” number of fault steps each with dip θ_j and net-slips n_j (j = 1 to m), for an oblique-slip reverse fault with sinistral slip component,

$$I_{F1}: [x_i - \sum n_j \cos\Phi_j, y_i + \sum n_j \sin\Phi_j.\cos\theta_j, z_i - \sum n_j \cos\Phi_j.\cos\theta_j] \quad (40)$$

Similarly one can write expressions for other oblique-slip fault patterns with multiple fault steps.

2.2. Faulting involving rotation of faulted block

2.2.1. Rotational fault

In Fig. 3a1, consider O (0, y_1 , z_1) be the fixed pivot about which a clock-wise sense of rotation of the rear faulted block (footwall block: block-B) takes place in terms of absolute rotation of the other block (hangingwall block: block-A). Recognizing faulted blocks as block-A and block-B is necessary in this article since the case of horizontal fault plane will also be referred in “Section 3: Discussions” where the faulted blocks cannot be recognized as the hangingwall block or the footwall block. Consider O be the one of the terminal points of the fault trace. Such a fault has been described as a “hinge fault” by Donath (1962) but a “scissor fault” by Roberts (1982). The axis of rotation is a line passing through O and is perpendicular to the fault plane. Recalling that eqn (3) represents the fault plane, the equation of the axis is:

$$(y_1 - y) \cot \theta = (z_1 - z) \quad (41)$$

Say the angle $\text{POP}'' = \omega$. The co-ordinate of P'' in the hangingwall block (block-A in Fig. 3a1) will be deduced in two steps. Consider a vertical plane Y = y_1 , parallel to the XZ plane, passing through PO (Fig. 3a2). Say OP rotates downward about the point O to OP'. Co-ordinate of P' will be first obtained. After that the plane $y = y_1$ will be rotated about the OP axis so that it coincides with the given fault plane. After rotation P' will coincide with P''. Geometrically, the co-ordinate of P' after such a rotation will be deduced.

Line P'N is drawn perpendicular to the line OP. Length $OP = x_p = OP'$. Now in triangle NP'O, length $NP' = OP' \sin \omega$, or

$$NP' = x_p \sin \omega \quad (42)$$

In the same way, length $NO = x_p \cos \omega$. Therefore the P' coordinate is $[x_p \cos \omega, y_1, z_1 - x_p \sin \omega]$. Now consider a vertical plane passing through N and parallel to the XZ plane, i.e., $y = x_p \cos \theta$. Now the line NP' will be rotated keeping N as the fixed point so that line NP plunges θ and trend in the same direction as the dip direction of the fault plane (in this case the positive side of the Y-axis). By rotating like this, P' will coincide with P''. Note $NP' = NP''$ since NP rotates to a new position NP''. Therefore from eqn (42),

$$NP'' = x_p \sin \omega \quad (43)$$

With reference to Fig. 3a3, drop a perpendicular P''T on the line NP'. In triangle P''TN, $NT = NP'' \sin \theta$. Substituting NP'' from eqn (43),

$$NT = x_p \sin \omega \sin \theta \quad (44)$$

$$\text{Now } TP' = (NP' - NT) = x_p \sin \omega - x_p \sin \omega \cos \theta \quad (45)$$

Again, from triangle P''TN, $TP'' = NP'' \cos \theta$. Substituting NP'' from eqn (43),

$$TP'' = x_p \sin \omega \cos \theta \quad (46)$$

By rotating the NP' line in this specific way, the x-ordinate of P' point in its new position P'' remains the same, but the y-ordinate increases by TP'' distance (see eqn (46)), and the Z-ordinate increases by TP' distance (see eqn (45)).

Therefore the P'' coordinate is $[x_p \cos \omega, y_1 + x_p \sin \omega \cos \theta,$

$$z_1 - x_p \sin \omega \sin \theta] \quad (47)$$

Therefore, any point in the block-A, $[r_i]$ ($r = x, y, z$) after the absolute rotation of the block-A, attains the new co-ordinate $I_{\text{block-A1}}$:

$$[x_p \cos \omega, y_1 + x_p \sin \omega \cos \theta, z_1 - x_p \sin \omega \sin \theta] \quad (48)$$

Had there been a counter-clockwise sense of relative rotation attained by absolute rotation of the block-B alone, the coordinate $I_{\text{block-B1}}$ is

$$[x_p \cos \omega, y_1 - x_p \sin \omega \cos \theta, z_1 + x_p \sin \omega \sin \theta] \quad (49)$$

Exp (47) can be cross-checked in the following two ways. First, the distance between the points P $[x_p, y_1, z_1]$ and P'', given by the exp (47) itself, is found to be $1.4 \cdot x_p (1 - \cos \omega)$ as per the formula of finding distance between two points in 3D geometry. This matches with the trigonometric way of deducing PP'' distance from the triangle OPP'' that lies on the fault plane (where distance $OP = \text{distance } OP'' = x_p$, and angle $\text{POP}'' = \omega$). Second, note that for the pivot itself (0, y_1, z_1) for which $x_p = 0$, the point after rotation attains the position, after substituting $x_1 = x_p = 0$ in exp (47), is (0, y_1, z_1), which is the same as its original position. This is as expected.

In case, the pivot does not lie at the either of the end points of the fault strike, but rests in between (Fig. 3b; “pivotal fault” as per Donath, 1962), the first few steps of deduction of P'' co-ordinate remains the same. For all points P_b for which its x-ordinate (x_{pb}) is more than that of the pivot (x_1), i.e., $x_{pb} > x_1$, after rotational faulting, its new position P'' will be:

$$[x_{pb} \cos \omega, y_1 + x_{pb} \sin \omega \cos \theta, z_1 - x_{pb} \sin \omega \sin \theta] \quad (50)$$

This is same expression as exp (48) but with $x_p = x_{pb}$ substituted.

For all points P_s for which the x-ordinate (x_{ps}) is less than that of the pivot (x_1), i.e., $x_{ps} < x_1$, after rotational faulting, its new position P'' will be:

$$[x_{ps} \cos \omega, y_1 - x_{ps} \sin \omega \cos \theta, z_1 - x_{ps} \sin \omega \sin \theta] \quad (51)$$

2.2.2. Roto-translational fault

Two broad types of faulting can be possible under this category: (i) rotation and translation of faulted block happen simultaneously; (ii) first only a translation takes place and then a purely rotation happens (Fig. 3c), (iib) or vice versa. In cases (iia) and (iib), say the total amount of anti-clockwise rotation (ω) of such a faulted block happens when the footwall block (block-B) remain stationary and the hangingwall block (block-A) only rotates. Block-A also translates like an oblique-slip normal fault with a net-slip “n” with a pitch of “ Φ ”. In such a case, I_{H1} is given by the sum of the respective ordinates for I_{H1} for a pure translational oblique-slip normal fault with sinistral slip component (case of Fig. 1d and exp (14)) and that for a pure rotational fault (case of Fig. 3a1, exp (52)):

$$I_{\text{H1}} [x_p \cos \omega - n \cos \Phi, y_1 + \cos \theta (x_p \sin \omega + n \sin \Phi), z_1 - \sin \theta (n \sin \Phi - x_p \sin \omega)] \quad (52)$$

Similarly one can work out I_{F1} when only the hangingwall and when only the footwall block slips and rotates. One can also find out various simpler cases, such as a purely strike or purely a dip-slip component of translational slip by putting $\Phi = 0$ or 90° .

3. Discussions

For a vertical fault plane ($\theta = 90^\circ$ applied on exps. (14)–(18)) that can be either related to isostatic adjustment or strike slip tectonics, i.e., parallel to the XZ-plane, with equation $y = k$, terms such as normal fault, reverse fault, hangingwall block (block-A) and footwall block (block-B) do not apply. The co-ordinates of points after faulting, however, can still be worked out. For example, the co-ordinate of any point in the faulted “block-A” that move upward maintaining a sinistral slip component is given by $I_{\text{A1}} [x_i - n \cos \Phi, y_i, z_i - n \sin \Phi]$. It can be obtained by putting $\theta = 90^\circ$ in exp. (14) in Section 2.1.1.3.

Similarly, when the fault plane is horizontal, as happens locally in undulating fault planes (regional thrusts in collisional mountains and normal faults), putting, $\theta = 0$ in exp. (14) in Section 2.1.1.3, the shifted co-ordinate of the top block is given by $I_{\text{T1}} [x_i - n \cos \Phi, y_i - n \sin \Phi, z_i]$.

In case of fault planes with steps, note that exps. (19)–(40) remains unchanged if $\theta_2 < \theta_1$, since $\cos(-\alpha) = \cos(\alpha)$. Secondly, in exps. (20)–(41), by choosing few $\theta_i = 0$, one can work out the flat-ramp-flat

(Davis et al., 2012), the flat-ramp-flat-ramp (Lock, 2007), the ramp-flat-ramp cases (Ehrlich and Gabrielsen, 2004; Padrera et al., 2012).

Mukherjee and Khonsari (2017) define “effective-slip” (n_{eff}) for non-planar and/or non-translational faulting. For such faults, it is the linear distance between two originally coincident points before faulting that are now separated by the process of faulting. For such faults, net-slip > effective-slip. For translational faults with a single planar fault surface, net-slip = effective-slip. For dip-slip normal faults with two steps, linear distance $PP_2 = n_{\text{eff}}^2$ from Fig. 2a2,

$$n_{\text{eff}}^2 = [n_{d1}^2 n_{d2}^2 + 2 \cdot n_{d1} \cdot n_{d2} \cdot \text{Cos}(\theta_1 - \theta_2)]^{0.5} \quad (53)$$

Eqn (53) is cross-checked to be correct since the linear distance between the points P [x_1, y_1, z_1] and P₂ (coordinate as per exp. (21)) matches with eqn (53).

This work utilizes purely a 3D geometric approach and does not bring solid mechanics in tracking particles in the faulted blocks. 3D geometric approach can be found in many classic structural geology articles e.g., Ramsay (1980) in the context of ductile shear zones, and McNaught and Mitra (1996) while balancing cross-sections.

Allmendinger et al. (2012) converted several structural geological problems and their solutions into 3D co-ordinate geometrical exercises. Such an approach helps to write computer programs for complicated deformations. The present article does the first part of the work, i.e.,

Repository

Derivation of equation of fault plane as presented in eqn (2) in the main text:

With reference to Fig. 1 in the main text, say the fault plane has an equation:

$$ax + by + cz + d = 0 \quad (1)$$

Since the plane cuts the three co-ordinate axes at positive sides and does not pass through the origin [0,0,0], a, b, c > 0 and d < 0.

As this plane passes through P (x_1, y_1, z_1) and Q (0, y_1, z_1),

$$a = 0 \quad (2)$$

Equation of XY-plane is:

$$z = 0 \quad (3)$$

Angle between the XY-plane and the fault plane is the dip (θ) of the fault plane.

$$\text{Therefore, } \text{Cos}\theta = c / (b^2 + c^2)^{0.5} \quad (4)$$

Simplifying,

$$b = \pm c \tan\theta \quad (5)$$

From eqns (1), 2 and 5, after eliminating a and b, possible equations of the fault plane:

$$z = -d \cdot c^{-1} \pm y \cdot \tan\theta \quad (6)$$

Out of these two possibilities, is always > 0 for all y > 0, since d < 0 and c > 0. Therefore eqn (7) represents the fault plane as shown in Fig. 1.

$$z = -d \cdot c^{-1} + y \cdot \tan\theta \quad (7)$$

After applying the standard formula between two planes: the fault plane (eqn (7)) and the XY-plane (eqn (3)), θ angle is found. This confirms that eqn (7) is certainly correctly deduced.

Appendix A. Supplementary data

Supplementary data to this article can be found online at <https://doi.org/10.1016/j.marpetgeo.2019.05.037>.

References

- Allmendinger, R.W., Cardozo, N., Fisher, D.M., 2012. Structural Geology Algorithms: Vectors and Tensors. Cambridge University Press, 978-1-107-01200-4pp. 1–289.
- Ando, E., Hall, S.A., Viggiani, G., Desrues, J., Besuelle, P., 2012. Grain-scale experimental investigation of localised deformation in sand: a discrete particle tracking approach. Acta Geotechnica 7, 1–13.
- Billings, M.P., 1972. Structural Geology, third ed. Prentice-Hall of India Pvt. Ltd, pp. 178.
- Boyer, S.E., Elliot, D., 1982. Thrust systems. AAPG Bull. 66, 1196–1230.
- Cunningham, W.D., Mann, P., 2007. Tectonics of strike-slip restraining and releasing bends. In: In: Cunningham, W.D., Mann, P. (Eds.), Tectonics of Strike-Slip Restraining and Releasing Bends, vol. 290. Geological Society, London, Special Publications, pp. 1–12.
- Cobbold, P.R., Quinquis, H., 1980. Development of sheath folds in shear regimes. J. Struct. Geol. 2, 119–126.
- Dasgupta, S., Mukherjee, S., 2017. Brittle shear tectonics in a narrow continental rift: asymmetric non-volcanic Barmer basin (Rajasthan, India). J. Geol. 125, 561–591.
- Davis, G., Reynolds, S.J., Kluth, C.F., 2012. Structural Geology of Rocks and Regions, third ed. John Wiley & Sons, New York 978-0-471-15231-6.
- Donath, F.A., 1962. Analysis of basin-range structure, south-central Oregon. Geol. Soc. Am. Bull. 73, 1–16.
- Ehrlich, R., Gabrielsen, R.H., 2004. The complexity of a ramp-flat-ramp fault and its hanging wall structuring: an example from the Njard oil field, offshore mid-Norway.

new geometric formulation of fault slip studies. The numerical introduced in this article will be simple to follow for the geosciences students who have taken a course on 3D coordinate geometry. Therefore the instruction can teach this article while introducing different kinds of faults in block diagrams.

Particle tracking by 3D co-ordinate geometry needs also be extended for listric fault planes with strike-slip, dip-slip and oblique-slip patterns. Listric faults have been modeled alternately as spherical surfaces/circular arcs (e.g., Schultz, 1987; 1992; Mukherjee and Agarwal, 2018), cylindrical geometry (Ellis and McClay, 1988) and Lohr et al. (2008). Such a simplified assumption can be adopted in the present case.

Acknowledgements

SM thanks his Ph.D. students Narayan Bose and Dripta Dutta for always assisting, even in their respective final years of thesis submission. Additional thanks to Narayan Bose for making a critical partial internal review. Funded by CPDA grant of IIT Bombay to SM. The anonymous reviewer is thanked for positive yet intense comments. The Handling Editor Prof. Adam Bumby is thanked for his efficient work. This article was written on a wheelchair. Thanks to my wife Payel Mukherjee for all the assistance.

- Petrol. Geol. 10, 305–317.
- Ellis, P.G., McClay, K.R., 1988. Listric extensional fault systems - results of analogue model experiments. *Basin Res.* 1, 55–70.
- Fossen, H., 2016. *Structural Geology*, second ed. Cambridge University Press, pp. 386–387 13: 978-1107057647.
- Ghosh, S.K., 1993. *Structural Geology: Fundamentals and Modern Developments*. Pergamon Press, pp. 429.
- Gibbs, A.D., 1984. Structural Evolution of extensional basin margins. *J. Geol. Soc. London* 141, 609–620.
- Groshong Jr., R.H., 2006. *3D Structural Geology: A Practical Guide to Quantitative Surface and Subsurface Map Interpretation*. Springer, Berlin, pp. 1–382 10 3-540-31054-1.
- Huetra, A.D., Rodgers, D.W., 1996. Kinematic and dynamic analysis of a low-angle strike-slip fault: the Lake Creek fault of south-central Idaho. *J. Struct. Geol.* 18, 585–593.
- Kent, W.N., Hickman, R.G., Dasgupta, U., 2002. Application of a ramp/flat-fault model to interpretation of the Naga thrust and possible implications for petroleum exploration along the Naga thrust front. *AAPG Bull.* 86, 2023–2045.
- Kobayashi, T., Morishita, T., Yarai, H., 2018. SAR-revealed slip partitioning on a bending fault plane for the 2014 Northern Nagano earthquake at the northern Itoigawa–Shizuoka tectonic line. *Tectonophysics* 733, 85–99.
- Lock, J., 2007. *Interpreting Low-Temperature Thermochronometric Data in Fold-And-Thrust Belts: an Example from the Western Foothills, Taiwan*. Ph.D. Thesis. University of Washington, pp. 131.
- Lohr, T., Krawczyk, C.M., Oncken, O., Tanner, D.C., 2008. Evolution of a fault surface from 3D attribute analysis and displacement measurements. *J. Struct. Geol.* 30, 690–700.
- Lopez-Mir, B., 2019. Cross-section construction and balancing: examples from the Spanish Pyrenees. In: Billi, A., Fagereng, A. (Eds.), *Problems and Solutions in Structural Geology and Tectonics*. Series Editor: S. Mukherjee. *Developments in Structural Geology and Tectonics*. Elsevier9780128140482, .
- McClay, K., 1990. Deformation mechanics in analogue models of extensional fault systems. In: Knipe, R.J., Rutter, E.H. (Eds.), *Deformation Mechanisms, Rheology and Tectonics*, vol. 54. Geological Society Special Publication, pp. 445–453.
- Marshak, S., Mitra, G., 1988. *Basic Methods of Structural Geology*. Prentice-Hall 10: 0130651788.
- McNaught, M., Mitra, G., 1996. The use of finite strain data in constructing a retro deformable cross section of the Meade thrust sheet, southeastern Idaho. *J. Struct. Geol.* 18, 573–583.
- Merle, O., 1998. *Emplacement Mechanism of Nappe and Thrust Sheets*. Kluwer Academic Publishing, Dordrecht, pp. 12.
- Misra, A.A., Bhattacharya, G., Mukherjee, S., Bose, N., 2014. Near N-S paleo-extension in the western Deccan region in India: does it link strike-slip tectonics with India-Seychelles rifting? *Int. J. Earth Sci.* 103, 1645–1680.
- Mukherjee, S., 2013. Channel flow extrusion model to constrain dynamic viscosity and Prandtl number of the Higher Himalayan Shear Zone. *Int. J. Earth Sci.* 102, 1811–1835.
- Mukherjee, 1988. Airy's isostatic model: a proposal for a realistic case. *Arab. J. Geosci.* 10, 268.
- Mukherjee, S., 2018. Moment of inertia for rock blocks subject to bookshelf faulting with geologically plausible density distributions. *J. Earth Syst. Sci.* 127, 80.
- Mukherjee, S., 2019. Kinematics of pure shear ductile deformation within rigid walls: new analyses. In: Billi, A., Fagereng, A. (Eds.), *Problems and Solutions in Structural Geology and Tectonics*. Series Editor: Mukherjee S. *Developments in Structural Geology and Tectonics Book Series*. Elsevier9780128140482, .
- Mukherjee, S., Agarwal, I., 2018. Shear heat model for gouge free dip-slip listric normal faults. *Mar. Pet. Geol.* 98, 397–400.
- Mukherjee, S., Khonsari, M.M., 2017. Brittle rotational faults and the associated shear heating. *Mar. Pet. Geol.* 88, 551–554.
- Mukherjee, S., Khonsari, M.M., 2018. Inter-book normal fault-related shear heating in brittle bookshelf faults. *Mar. Pet. Geol.* 97, 45–48.
- Mukherjee, S., Tayade, L., 2019. Kinematic analyses of brittle roto-translational planar and listric faults based on various rotational to translational velocities of the faulted blocks. *Mar. Pet. Geol.* <https://doi.org/10.1016/j.marpetgeo.2019.04.024>.
- Nemser, E.S., Kowan, D.S., 2009. Down-dip segmentation of strike-slip fault zones in the brittle crust. *Geology* 37, 419–422.
- Padrera, A., Galindo-Zaldívar, J., Lamas, F., Ruiz-Constan, A., 2012. Evolution of near-surface ramp-flat-ramp normal faults and implication during intramontane basin formation in the eastern Betic Cordillera (the Huércal-Overa Basin, SE Spain). *Tectonics* 31, TC4024.
- Ramsay, J.G., 1980. Shear zone geometry: a review. *J. Struct. Geol.* 2, 83–99.
- Roberts, J.L., 1982. *Introduction to Geological Maps and Structures*. Pergamon Press, Oxford, pp. 137.
- Rodriguez-Castaneda, J., 1996. Late-Jurassic and mid-Tertiary brittle-ductile deformation in the Opodepe region, Sonora, Mexico. *Revista Mexicana de Ciencias Geológicas* 13, 1–9.
- Savage, H.M., Cooke, M.L., 2003. Can flat-ramp-flat fault geometry be inferred from fold shape?: a comparison of kinematic and mechanical folds. *J. Struct. Geol.* 25, 2023–2034.
- Schultz, R.A., 1992. Mechanics of curved slip surfaces in rock. *Eng. Anal. Bound. Elem.* 10, 147–154.
- Schultz, R.A., 1987. *Mechanics of Curved Strike-Slip Faults*. Ph.D. thesis. Purdue University, pp. 1–142.
- Turcotte, D.L., Schubert, G., 2002. *Geodynamics*, second ed. Cambridge University Press, Cambridge.